Journal of Materials Chemistry B

ROYAL SOCIETY OF CHEMISTRY

PAPER

View Article Online
View Journal | View Issue

Cite this: J. Mater. Chem. B, 2024, 12, 6128

Fluorinated BPA derivatives enhanced ^{10}B delivery in tumors†

Dandan Ding,[ad] Shushan Mo,[ac] Qishan Li,[ab] Fei Wang,[ad] Xueyi Wang,*[ad] Caiwen Ou*[a] and Zhenhua Li *[ad]

Received 18th April 2024,
Accepted 20th May 2024

DOI: 10.1039/d4tb00846d

rsc.li/materials-b

Boron neutron capture therapy (BNCT) is an emerging approach for treating malignant tumors with binary targeting. However, its clinical application has been hampered by insufficient ^{10}B accumulation in tumors and low ^{10}B concentration ratios of tumor-to-blood (T/B) and tumor-to-normal tissue (T/N). Herein, we developed fluorinated BPA derivatives with different fluorine groups as boron delivery agents for enabling sufficient ^{10}B accumulation in tumors and enhancing T/B and T/N ratios. Our findings demonstrated that fluorinated BPA derivatives had good biological safety. Furthermore, fluorinated BPA derivatives showed improved ^{10}B accumulation in tumors and enhanced T/B and T/N ratios compared to the clinical boron drug fructose-BPA (f-BPA). In particular, in B16-F10 tumor-bearing mice, fluorinated BPA derivatives met the requirements for clinical BNCT even at half of the clinical dose. Thus, fluorinated BPA derivatives are potentially effective boron delivery agents for clinical BNCT in melanoma.

1. Introduction

Boron neutron capture therapy (BNCT) is an emerging radiotherapy with binary targeting properties, which was clinically approved in Japan in 2020 and exhibited excellent efficacy in inhibiting locally aggressive tumors.[1–4] The high-energy alpha particles (^{4}He) and lithium-7 (^{7}Li) nuclei released during BNCT can selectively destroy cancer cells without damaging the surrounding normal tissues due to the killing range (5–9 μm) of these nuclei being approximately the diameter of the cells.[5,6] Clinical trials showed that BNCT had been the most promising treatment for infiltrative, diffuse, and metastatic tumors, including glioblastoma, malignant melanoma, and recurrent head and neck cancers.[7–11]

Successful BNCT relies on the capture of thermal neutrons by ^{10}B in tumor cells.[12] Therefore, the key to BNCT drug development is to realize the highly selective ^{10}B accumulation in tumor cells. Ideal boron delivery agents require the following conditions, such as the ^{10}B concentration ratios of tumor-to-blood (T/B) and tumor-to-normal tissue (T/N) being not less than 3 (T/B > 3 : 1 and T/N > 3 : 1), sufficient ^{10}B contents (>20 μg ^{10}B per g tumor) in tumor cells, rapid clearance from blood and normal tissues, and prolonged retention time in the tumor.[13–15] Currently, only two boron compounds, 4-boronophenylalanine (BPA) and disodium mercaptoundecahydro-*closo*-dodecaborate (BSH), are approved to apply in clinical BNCT trials.[16–19] Although BSH has a higher boron content, its tumor specificity is relatively poor. A large number of studies have demonstrated that BPA can selectively enter into cancer

[a] The Tenth Affiliated Hospital, Southern Medical University (Dongguan People's Hospital), Dongguan 523059, China. E-mail: ixueyi@smu.edu.cn, oucaiwen@smu.edu.cn, zhenhuali@hbu.edu.cn
[b] The First School of Clinical Medicine, Southern Medical University, Guangzhou, Guangdong 510515, China
[c] College of Pharmaceutical Science, Key Laboratory of Pharmaceutical Quality Control of Hebei Province, Hebei University, Baoding 071002, China
[d] Guangdong Provincial Key Laboratory of Cardiac Function and Microcirculation, Guangdong 510515, China

† Electronic supplementary information (ESI) available. See DOI: https://doi.org/10.1039/d4tb00846d

Zhenhua Li

Dr. Zhenhua Li completed his doctorate in inorganic chemistry at Changchun Institute of Applied Chemistry, Chinese Academy of Sciences in 2015. After postdoc training at the Joint Department of Biomedical Engineering, University of North Carolina (UNC) at Chapel Hill and North Carolina State University, he joined the 10th affiliated Hospital, Southern Medical University. His research focuses on the design of biomimetic materials for cancer therapy and regenerative medicine.

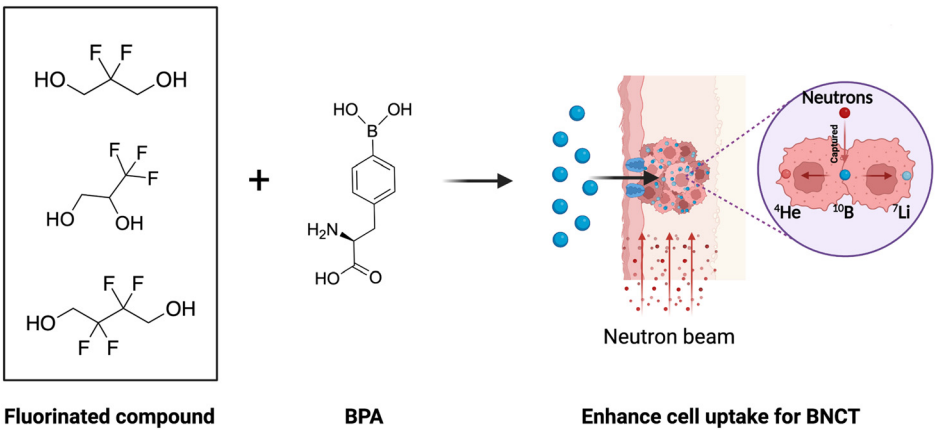

Fig. 1 Schematic illustration of fluorinated BPA derivatives enhancing the ^{10}B accumulation in tumors *in vivo*. The figure was created with BioRender.com.

cells by the overexpressed L-amino acid transporter-1 (LAT-1) in tumor cells due to the structure of phenylalanine.[20,21] But BPA has poor water solubility and fructose is utilized to increase the aqueous solubility of BPA by binding to the boric acid of BPA for clinical applications.[22–24] Nonetheless, insufficient ^{10}B accumulation in tumors and low T/B ratios are still the main reasons limiting the effectiveness of BNCT.[14] Therefore, it is crucial to develop novel boron drugs which can increase the ^{10}B concentration in tumor cells and enhance T/B and T/N ratios for BNCT treatment.

Recent studies have shown that the presence of fluorocarbon bonds can improve the permeability of cell membranes and the pharmacokinetic properties of drugs leading to enhanced drug uptake in tumor cells.[25–28] Fluorine substituents have been common ingredients in drugs in recent decades, especially in oncology applications, where approximately 50% of marketed drugs are fluorinated, including a variety of antitumor drugs.[29,30] Besides, fluorine can increase the affinity for natural receptors and improve metabolic stability due to its polar hydrophobicity, thereby enhancing drug availability.[31] Metelev *et al.* reported the synthesis of fluorocarbon-based oligodeoxynucleotide duplexes (ODND) and demonstrated a significant increase in cellular uptake after modification with fluorocarbons. Thus, it is believed that the high affinity of modification with fluorocarbons for cell membranes contributes to enhanced intracellular uptake.[32]

Based on these, in this work, we synthesized fluorinated BPA derivatives with different fluorine groups by a simple method to investigate their ^{10}B delivery efficiency in both glioblastoma and melanoma models commonly used in clinical BNCT (Fig. 1). Our findings indicated that the cellular uptake of fluorinated BPA derivatives was higher than that of f-BPA in both GL261 and B16-F10 tumor cells and was in accordance with the requirement of BNCT ($>10^9$ ^{10}B per cell, *i.e.*, 16.67 ng ^{10}B per 10^6 cells). Notably, the ^{10}B uptake in B16-F10 cells was higher than that in GL261 cells. Moreover, fluorinated BPA derivatives demonstrated higher ^{10}B accumulation in tumors and higher T/B and T/N ratios than f-BPA in GL261 and B16-F10 tumor-bearing mice, whereas they showed insufficient ^{10}B uptake in GL261 tumor-bearing mice according to the BNCT requirement (>20 μg ^{10}B per g tumor). In contrast, in B16-F10 tumor-bearing mouse models, the ^{10}B content in tumors reached 39.78 ± 4.52 ng g^{-1} tumor for 2F-BPA, 40.20 ± 2.83 ng g^{-1} tumor for 3F-BPA, and 38.42 ± 3.28 ng g^{-1} tumor for 4F-BPA, significantly surpassing the requirements for ^{10}B content in tumors. Furthermore, the biosafety of F-containing drugs is of great concern, and the results of our safety experiments showed that fluorinated BPA derivatives had better biocompatibility in GL261 and B16-F10 cells and had no significant systemic toxicity *in vivo*. Therefore, fluorinated BPA derivatives have great potential to become efficient boron delivery agents in malignant melanoma for clinical BNCT.

2. Materials and methods

2.1. Materials and characterization

^{10}BPA was purchased from Sunshine Lake Pharma Co., Ltd (China). Fructose was purchased from Aladdin Chemical Reagent Co., Ltd (China). 2,2-difluoropropane-1,3-diol, 2,2-difluoropropane-1,3-diol, and 2,2,3,3-tetrafluorobutane-1,4-diol were purchased from Bidepharm (China). HNO_3 was purchased from Damao. The cell counting kit-8 (CCK-8) was purchased from Bioss Biotechnology Co., Ltd (China). All chemical reagents were used directly without additional purification. ^{1}H nuclear magnetic resonance (NMR) spectra were measured using an Advance Neo 400 MHz spectrometer (Bruker). Electrospray ionization mass spectrometry (ESI-MS) was conducted using an ISQ EM model (Thermo Scientific) mass spectrometer. The ^{10}B contents were analyzed by ICP-MS (Thermo Scientific).

2.2. Synthesis of fluorinated BPA derivatives

1 g of BPA was added into 10 mL of water with stirring, and then 1 M HCl was dropwise added into the BPA solution until the solution turned clear from turbid. Then BPA·HCl as a white powder was obtained after freeze-drying.

Small molecules with different fluorine groups and BPA·HCl (at a molar ratio of 1 : 1.5) were added into dry DMSO with stirring. After 24 h, the solution was mixed with water and filtered using 0.22 μm PES syringe filters. The final compounds

were obtained after freeze-drying and then characterized by ^{1}H NMR (D_2O) and ESI-MS.

(*S*)-2-Amino-3-(4-(5,5-difluoro-1,3,2-dioxaborinan-2-yl)phenyl)-propanoic acid (2F-BPA). ^{1}H NMR (400 MHz, D_2O) δ 7.68–7.63 (m, 2H), 7.28–7.22 (m, 2H), 4.15 (dd, J = 7.8, 5.5 Hz, 1H), 3.72 (t, J = 14.1 Hz, 4H), 3.25 (dd, J = 14.5, 5.6 Hz, 1H), 3.11 (dd, J = 14.5, 7.8 Hz, 1H).

ESI-MS: m/z calculated for $C_{12}H_{14}{}^{10}BF_2NO_4$, $[M + H]^+$ 285.1; found 285.0983.

(2*S*)-2-Amino-3-(4-(4-(trifluoromethyl)-1,3,2-dioxaborolan-2-yl) phenyl)propanoic acid (3F-BPA). ^{1}H NMR (400 MHz, D_2O) δ 7.48–7.42 (m, 2H), 7.12–7.07 (m, 2H), 3.53 (dd, J = 7.8, 5.1 Hz, 1H), 2.97 (dd, J = 13.7, 5.1 Hz, 1H), 2.76 (dd, J = 13.8, 7.8 Hz, 1H).

ESI-MS: m/z calculated for $C_{12}H_{13}{}^{10}BF_3NO_4$, $[M + H]^+$ 303.09; found 303.0888.

(*S*)-2-Amino-3-(4-(5,5,6,6-tetrafluoro-1,3,2-dioxaborepan-2-yl)phenyl)propanoic acid (4F-BPA). ^{1}H NMR (400 MHz, D_2O) δ 7.48–7.42 (m, 2H), 7.12–7.07 (m, 2H), 3.53 (dd, J = 7.8, 5.1 Hz, 1H), 2.97 (dd, J = 13.7, 5.1 Hz, 1H), 2.76 (dd, J = 13.8, 7.8 Hz, 1H).

ESI-MS: m/z calculated for $C_{13}H_{14}{}^{10}BF_4NO_4$, $[M + H]^+$ 335.1; found 335.0947.

2.3. Cell culture

GL261 (mouse glioma cells) cells and B16-F10 (mouse melanoma cells) cells were cultured in RPMI-1640 medium and DMEM containing 10% fetal bovine serum (Gibco) and 1% penicillin–streptomycin in a humidified atmosphere with 5% CO_2 at 37 °C, respectively.

2.4. *In vitro* cytotoxicity of fluorinated BPA derivatives

The cytotoxicity of fluorinated BPA derivatives was investigated using the CCK-8 kit. The GL261 cells and B16-F10 cells (5×10^3 cells per well) were seeded into 96-well plates and incubated overnight, respectively. The samples (f-BPA, 2F-BPA, 3F-BPA, and 4F-BPA) with different concentrations were added to the cells. After incubating for 24 h, the medium in each well was replaced with 100 μL of fresh medium containing 10 μL of CCK-8 for another 2 h incubation. The absorbance of the samples at 450 nm was detected with a multifunctional enzyme labeler.

2.5. Serum chemistry and hematological analysis

Female C57BL/6J mice aged 5–6 weeks were intravenously injected with f-BPA and fluorinated BPA derivatives of different doses (BPA: 188, 250, and 375 mg kg^{-1}). Blood samples were collected for serum chemistry and hematological analysis at day 3 post-injection.

2.6. *In vitro* cellular uptake of fluorinated BPA derivatives

GL261 and B16-F10 cells with a density of 1×10^6 cells per well were seeded into 6-well plates and grown overnight. The fresh medium containing various concentrations of fluorinated BPA derivatives was added into each well. After co-incubation for 3 h and 24 h, the cells were carefully washed three times with PBS solution to remove ^{10}B in the medium. The obtained cells were digested with HNO_3 and heated with a microwave-accelerated reaction system. The cellular ^{10}B concentration was measured by ICP-MS after diluting with deionized water.

2.7. Establishment of tumor-bearing mouse models

Female C57BL/6J mice aged 5–6 weeks were purchased from Sipeifu Biotechnology Co., Ltd (Beijing, China), and all animal experiments were approved by the Dongguan People's Hospital Ethics Committee and conducted following the Regulations for the Administration of Affairs Concerning Experimental Animals (P.R. China). GL261 and B16-F10 tumor-bearing mouse models were established by injecting subcutaneously with GL261 cells and B16-F10 cells (2×10^6 cells per mouse) in the right flank, respectively.

2.8. *In vivo* biodistribution of fluorinated BPA derivatives

When the tumors reached 50–100 mm^3 in volume, the tumor-bearing mice were randomly divided into 4 groups (n = 3): f-BPA, 2F-BPA, 3F-BPA, and 4F-BPA. The tumor-bearing mice were injected intravenously with fluorinated BPA derivatives (BPA: 250 mg kg^{-1}). The tumors, blood, and main organs including the heart, liver, spleen, lungs, and kidneys were collected at 2 h after injection. These organs and tissues were weighed and digested using HNO_3, followed by heating with a microwave-accelerated reaction system. The ^{10}B content was detected by ICP-MS after diluting with deionized water.

2.9. Statistical analysis

All experimental data were processed using GraphPad Prism v.8.3. The data are presented as mean ± standard deviation (SD). The significance of group differences was assessed by an ordinary one-way ANOVA test and a two-way ANOVA test with multiple comparisons. A p value of less than 0.05 was considered statistically significant ($^*p < 0.05$, $^{**}p < 0.01$, $^{***}p < 0.001$, and $^{****}p < 0.0001$).

3. Results and discussion

3.1. Synthesis and characterization of fluorinated BPA derivatives

Due to the difficulties in the development of ^{10}B delivery agents to fulfill such high requirements for BNCT, BPA is still the primary choice for clinical BNCT and is approved for marketing in Japan. To improve the water solubility and cellular uptake of BPA, we chose diol-containing fluorinated compounds to bind with BPA to form novel fluorinated BPA derivatives. These fluorinated BPA derivatives have the potential to improve the BPA delivery efficiency, including the accumulation in tumors, T/N ratio, and T/B ratio.

The fluorinated BPA derivatives were synthesized as shown in Fig. S1 (ESI†). (*S*)-2-Amino-3-(4-(5,5-difluoro-1,3,2-dioxaborinan-2-yl)phenyl)propanoic acid (2F-BPA), (2*S*)-2-amino-3-(4-(4-(trifluoromethyl)-1,3,2-dioxaborolan-2-yl)phenyl)propanoic acid (3F-BPA) and (*S*)-2-amino-3-(4-(5,5,6,6-tetrafluoro-1,3,2-dioxaborepan-2-yl)phenyl)propanoic acid (4F-BPA) were synthesized using 2,2-difluoropropane-1,3-diol, 2,2-difluoropropane-1,3-diol, and 2,2,3,3-tetrafluorobutane-1,4-diol with BPA·HCl to form boron ester

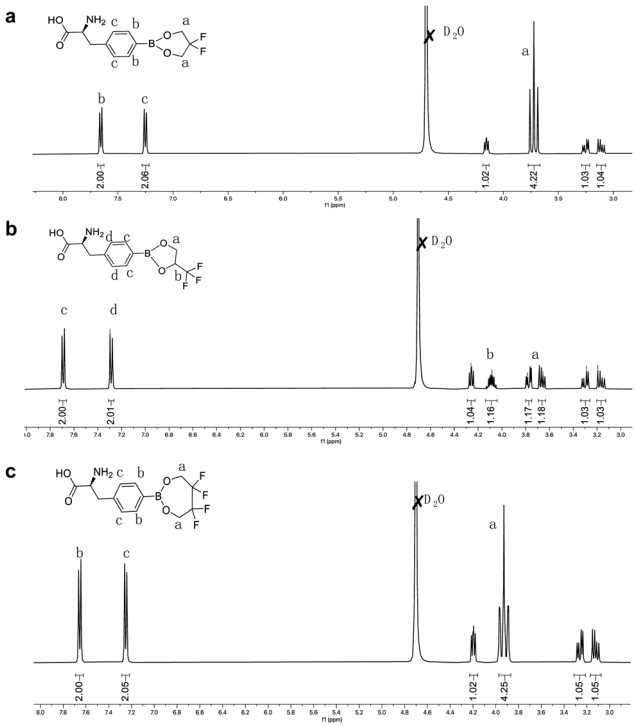

Fig. 2 ^{1}H NMR spectra of fluorinated BPA derivatives. The corresponding protons are marked in the structures of (a) 2F-BPA, (b) 3F-BPA, and (c) 4F-BPA.

bonds, respectively. In the procedure, the hydrochloride salt of BPA (BPA·HCl) was prepared and DMSO was chosen as the solvent for the reaction due to the poor solubility of BPA in water and organic solvents. After the reaction, the excess BPA was removed by repeated filtration in water. Finally, the pure fluorinated BPA derivatives were obtained after freeze-drying. As shown in Fig. 2 and Fig. S2 (ESI†), we characterized the fluorinated BPA derivatives using ^{1}H NMR and ESI-MS, indicating the successful preparation of fluorinated BPA derivatives. In detail, the integral ratios between the characteristic peaks in the fluorinated BPA derivatives, as depicted in Fig. 2, aligned precisely with the theoretical values. Moreover, compared to BPA (Fig. S3, ESI†), the hydrogen peaks on the benzene ring of the newly synthesized fluorinated BPA derivatives showed significant chemical shifts. In addition, fluorinated BPA derivatives had good water solubility at *in vivo* injectable doses.

3.2. Biological safety of fluorinated BPA derivatives

Cytotoxicity is an essential indicator for assessing drug biocompatibility.[33] We evaluated the cytotoxicity of fluorinated BPA derivatives in GL261 and B16-F10 tumor cells using the cell counting kit-8 (CCK-8) assay. Various concentrations of fluorinated BPA derivatives and f-BPA were added into GL261 and B16-F10 cells and incubated for 24 h. As shown in Fig. 3a–d, the cell viability of GL261 tumor cells with fluorinated BPA derivatives and f-BPA remained over 90%, even up to 50 ppm of the ^{10}B concentration. Similarly, the cell viability of B16-F10 tumor cells also showed a comparable level (Fig. 3e–h). In sum, the CCK-8 assay results suggested that fluorinated BPA derivatives, like f-BPA, exhibited excellent biocompatibility in both B16-F10 and GL261 tumor cells. We also evaluated the biosafety of fluorinated BPA derivatives by cell proliferation. After 72 h incubation of GL261 and B16-F10 cells with f-BPA and fluorinated BPA derivatives, there was no significant change in the cell number in various groups compared to the

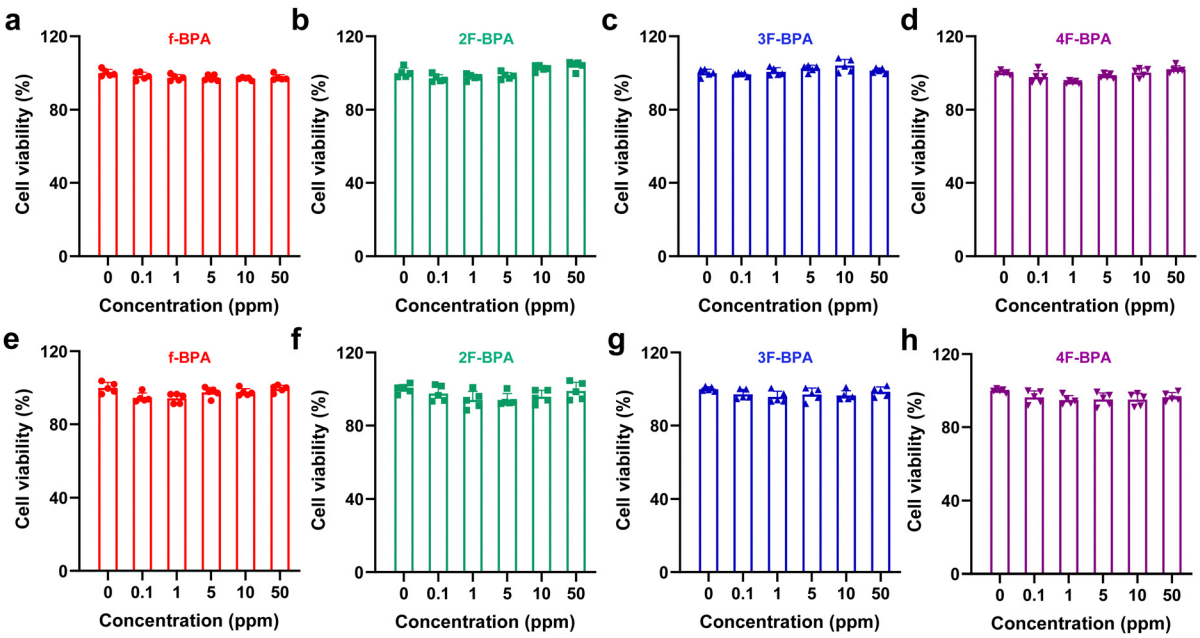

Fig. 3 The cytotoxicity of f-BPA and fluorinated BPA derivatives at different concentrations measured using the CCK-8 assay: (a) f-BPA in GL261 cells, (b) 2F-BPA in GL261 cells, (c) 3F-BPA in GL261 cells, (d) 4F-BPA in GL261 cells, (e) f-BPA in B16-F10 cells, (f) 2F-BPA in B16-F10 cells, (g) 3F-BPA in B16-F10 cells and (h) 4F-BPA in B16-F10 cells.

Table 1 Serum chemistry of mice intravenously injected with f-BPA and fluorinated BPA derivatives (BPA: 250 mg kg^{-1}) at day 3 (n = 3)

	ALT (U L^{-1})	AST (U L^{-1})	BUN (mg dL^{-1})	CREA (μmol L^{-1})	UA (μmol L^{-1})	CK (U L^{-1})	LDH (U L^{-1})
Control	56.00 ± 10.19	185.87 ± 18.01	23.98 ± 3.60	20.68 ± 4.91	73.20 ± 1.40	1541.47 ± 96.75	602.38 ± 32.02
f-BPA	63.47 ± 5.10	213.37 ± 28.58	21.12 ± 5.18	22.50 ± 1.18	90.07 ± 22.25	1999.33 ± 201.95	885.56 ± 139.13
2F-BPA	56.06 ± 17.92	173.27 ± 32.98	29.20 ± 3.04	18.67 ± 1.74	73.28 ± 16.11	1470.12 ± 394.20	720.95 ± 74.08
3F-BPA	46.52 ± 3.92	100.11 ± 17.92	26.63 ± 5.98	18.73 ± 7.57	99.65 ± 38.44	1318.10 ± 149.96	690.32 ± 133.10
4F-BPA	48.94 ± 13.94	172.50 ± 41.65	21.00 ± 3.63	20.30 ± 2.50	63.69 ± 10.24	1580.17 ± 195.08	645.73 ± 63.95

control group, indicating that fluorinated BPA derivatives are relatively safe (Fig. S4, ESI†).

In addition, serum chemistry and hematological analysis are important indicators of biosafety.[34] We evaluated serum chemistry and blood indexes at day 3 post-intravenous injection with f-BPA and fluorinated BPA derivatives. As shown in Table 1 and Fig. S5 (ESI†), there were no significant changes in hepatic function, kidney function, myocardial enzymes, and blood indexes between the groups (including the control, f-BPA, 2F-BPA, 3F-BPA, and 4F-BPA) and they were all in the normal ranges. Similarly, there were no obvious changes in the lower and higher dose fluorinated BPA derivative groups (Tables S1, S2 and Fig. S7, S7, ESI†). Furthermore, there was no significant decrease in the body weights of the mice after intravenous injection of fluorinated BPA derivatives (Fig. S8, ESI†). These results indicated that fluorinated BPA derivatives had no significant systemic toxicity with excellent biological safety.

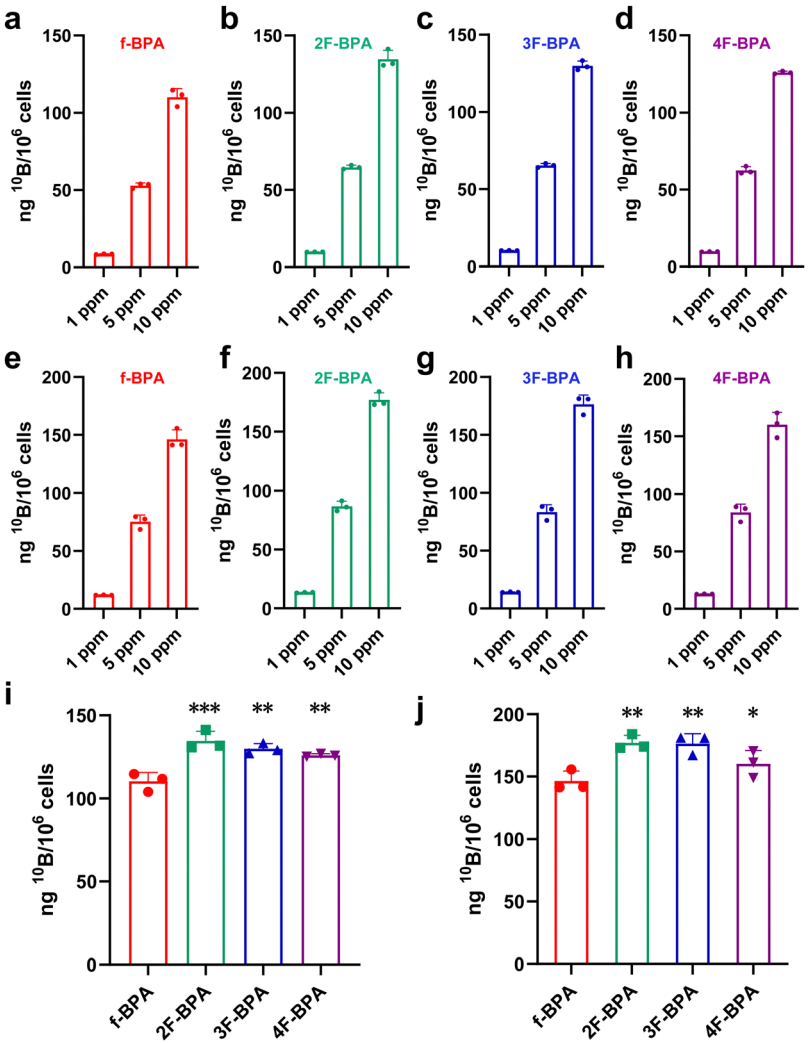

Fig. 4 *In vitro* cellular uptake of f-BPA and fluorinated BPA derivatives. The ^{10}B concentration in GL261 cells after 24 h incubation with various concentrations of (a) f-BPA, (b) 2F-BPA, (c) 3F-BPA and (d) 4F-BPA. The ^{10}B concentration in B16-F10 cells after 24 h incubation with various concentrations of (e) f-BPA, (f) 2F-BPA, (g) 3F-BPA and (h) 4F-BPA. (i) The ^{10}B concentration in GL261 cells after 24 h incubation with f-BPA, 2F-BPA, 3F-BPA and 4F-BPA at the same ^{10}B dose (10 ppm). (j) The ^{10}B concentration in B16-F10 cells after 24 h incubation with f-BPA, 2F-BPA, 3F-BPA and 4F-BPA at the same ^{10}B dose (10 ppm) (*$p < 0.05$, **$p < 0.01$, ***$p < 0.001$ compared with f-BPA).

We further evaluated the biosafety of fluorinated BPA derivatives by the hematoxylin and eosin (H&E) staining analysis. After the intravenous injection for 3 days, the major organs including the heart, liver, spleen, lungs, and kidneys were collected and sectioned. All groups showed no significant systemic toxicity to the major organs, implying that fluorinated BPA derivatives had good biosafety (Fig. S9, ESI†). Moreover, we also estimated the change of boron concentration in the blood of mice over time. As shown in Fig. S10 (ESI†), the boron concentration in the blood gradually decreased with time, indicating that the fluorinated BPA derivatives could be gradually metabolized.

3.3. *In vitro* cellular uptake of fluorinated BPA derivatives to enhance ^{10}B content

Sufficient ^{10}B contents (>16.67 ng ^{10}B per 10^6 cells) in tumor cells are vital for successful BNCT. To assess whether fluorinated BPA derivatives were effectively taken up into tumor cells, different concentrations of fluorinated BPA derivatives (1 ppm, 5 ppm, and 10 ppm) were co-incubated with GL261 and B16-F10 tumor cells, with f-BPA as the control. The ^{10}B concentrations in tumor cells were detected by inductively coupled plasma mass spectroscopy (ICP-MS). As shown in Fig. 4a–d, the ^{10}B contents in GL261 tumor cells gradually increased with concentration escalation of f-BPA and fluorinated BPA derivatives. The cellular uptake of f-BPA and fluorinated BPA derivatives also showed similar increasing trends in B16-F10 tumor cells (Fig. 4e–h). This result indicated a concentration-dependent uptake of ^{10}B in GL261 and B16-F10 tumor cells. In addition, the detection of ^{10}B by ICP-MS showed that f-BPA and fluorinated BPA derivatives could be rapidly taken up into tumor cells at 3 h and there was a significant increase at 24 h post-incubation, both in GL261 tumor cells (Fig. S11, ESI†) and in B16-F10 tumor cells (Fig. S12, ESI†).

In addition, we compared the cellular uptake of f-BPA and fluorinated BPA derivatives in GL261 tumor cells for 24 h at a ^{10}B concentration of 10 ppm. As shown in Fig. 4i, the average values of ^{10}B per 10^6 cells reached 110.13 ± 5.46 ng for f-BPA,

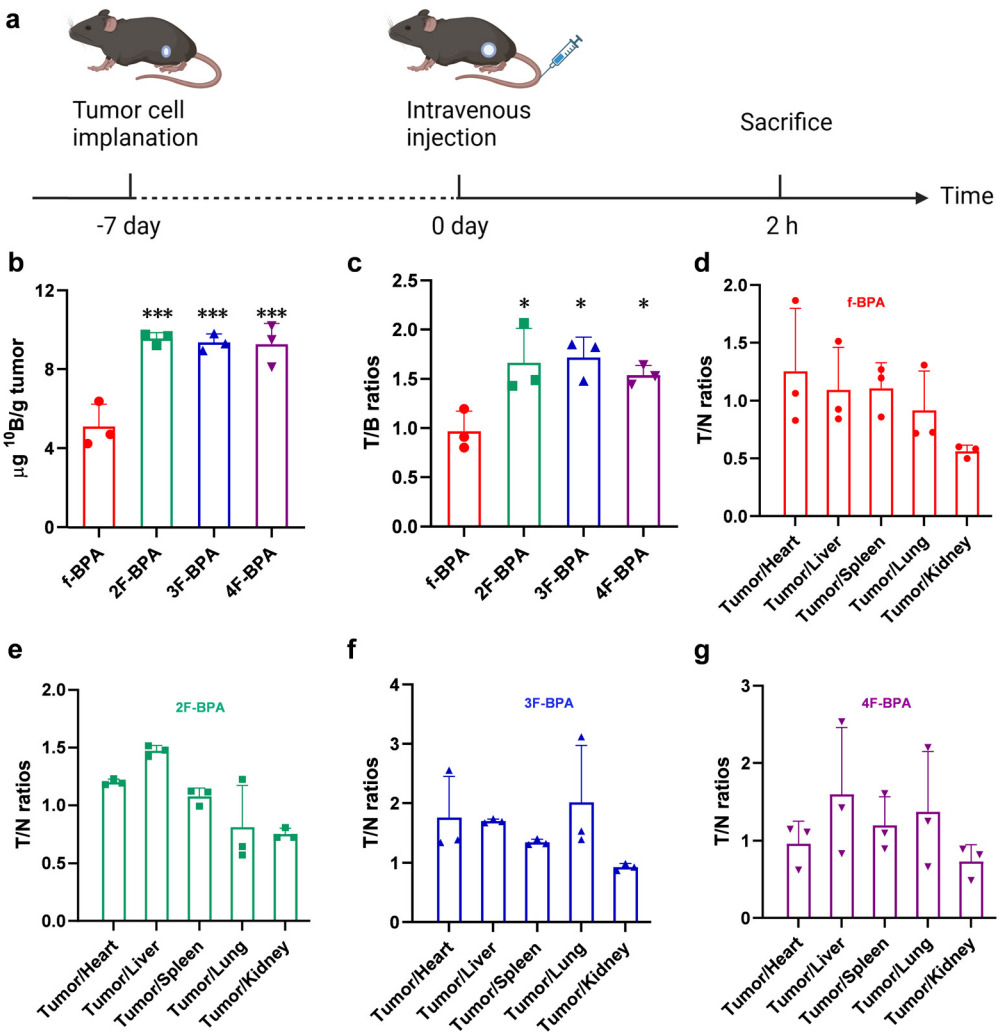

Fig. 5 *In vivo* biodistribution of f-BPA and fluorinated BPA derivatives at 2 h after intravenous injection for GL261 tumor-bearing mice. (a) Scheme of the experimental timeline. (b) The ^{10}B contents in tumors measured by ICP-MS for f-BPA, 2F-BPA, 3F-BPA and 4F-BPA. (c) Tumor-to-blood (T/B) ratios of f-BPA, 2F-BPA, 3F-BPA and 4F-BPA. Tumor-to-normal tissue (T/N) ratios (including the heart, liver, spleen, lungs, and kidneys) of (d) f-BPA, (e) 2F-BPA, (f) 3F-BPA and (g) 4F-BPA (ns > 0.05, *p < 0.05, **p< 0.01, ***p < 0.001 compared with f-BPA).

134.51 ± 5.81 ng for 2F-BPA, 129.83 ± 3.05 ng for 3F-BPA and 125.87 ± 0.89 ng for 4F-BPA, and the value exceeded the required ^{10}B content (16.67 ng per 10^6 cells) for BNCT. The concentration of ^{10}B in tumor cells with fluorinated BPA derivatives (including 2F-BPA, 3F-BPA, and 4F-BPA) was higher than that in tumor cells with f-BPA. In B16-F10 tumor cells, the mean ^{10}B content per 10^6 cells of f-BPA (146.44 ± 8.02 ng), 2F-BPA (177.06 ± 6.04 ng), 3F-BPA (176.43 ± 7.99 ng), and 4F-BPA (160.19 ± 10.80 ng) was also more than the required amount of ^{10}B for BNCT, and the cellular uptake of ^{10}B for fluorinated BPA derivatives was higher than that for f-BPA (Fig. 4j). Moreover, the cellular uptake of ^{10}B was higher in B16-F10 tumor cells than that in GL261 tumor cells. These results suggested that fluorinated BPA derivatives have a more pronounced advantage over f-BPA for ^{10}B delivery in GL261 and B16-F10 tumor cells. Therefore, fluorinated BPA derivatives may be better candidates to deliver sufficient ^{10}B into tumor cells.

3.4. *In vivo* biodistribution of fluorinated BPA derivatives to enhance the ^{10}B accumulation in tumors

The key to efficient BNCT is the accumulation of sufficient ^{10}B content (>20 μg ^{10}B per g tumor) in the tumor and high T/B and T/N ratios during neutron irradiation. To verify fluorinated BPA derivatives as potential boron delivery agents, we investigated whether fluorinated BPA derivatives could deliver sufficient ^{10}B to the tumor site and enhance the T/B and T/N ratios by intravenous injection of fluorinated BPA derivatives, with f-BPA as the control. The injection dose of ^{10}B was 250 mg kg^{-1} of BPA (equivalent to half of the clinical dose). The accumulation of ^{10}B in the tumor, blood, and various organs was measured by ICP-MS.

The *in vivo* distribution of f-BPA and fluorinated BPA derivatives in GL261 tumor-bearing mice was assayed at 2 h after intravenous injection (Fig. 5a), and the ^{10}B content of individual organs and blood is demonstrated in Fig. S13 (ESI†). As shown in Fig. 5b, the ^{10}B uptake in tumors reached 9.56 ± 0.30 ng per g tumor for 2F-BPA, 9.36 ± 0.43 ng per g tumor for 3F-BPA, and 9.27 ± 1.06 ng per g tumor for 4F-BPA. Although the ^{10}B content in the tumor did not reach the BNCT-requirements, fluorinated BPA derivatives still improved the ^{10}B accumulation in the tumor compared with f-BPA (5.12 ± 1.13 ng per g tumor). Surprisingly, the T/B ratio of fluorinated BPA derivatives (2F-BPA: 1.66 ± 0.35, 3F-BPA: 1.72 ± 0.21,

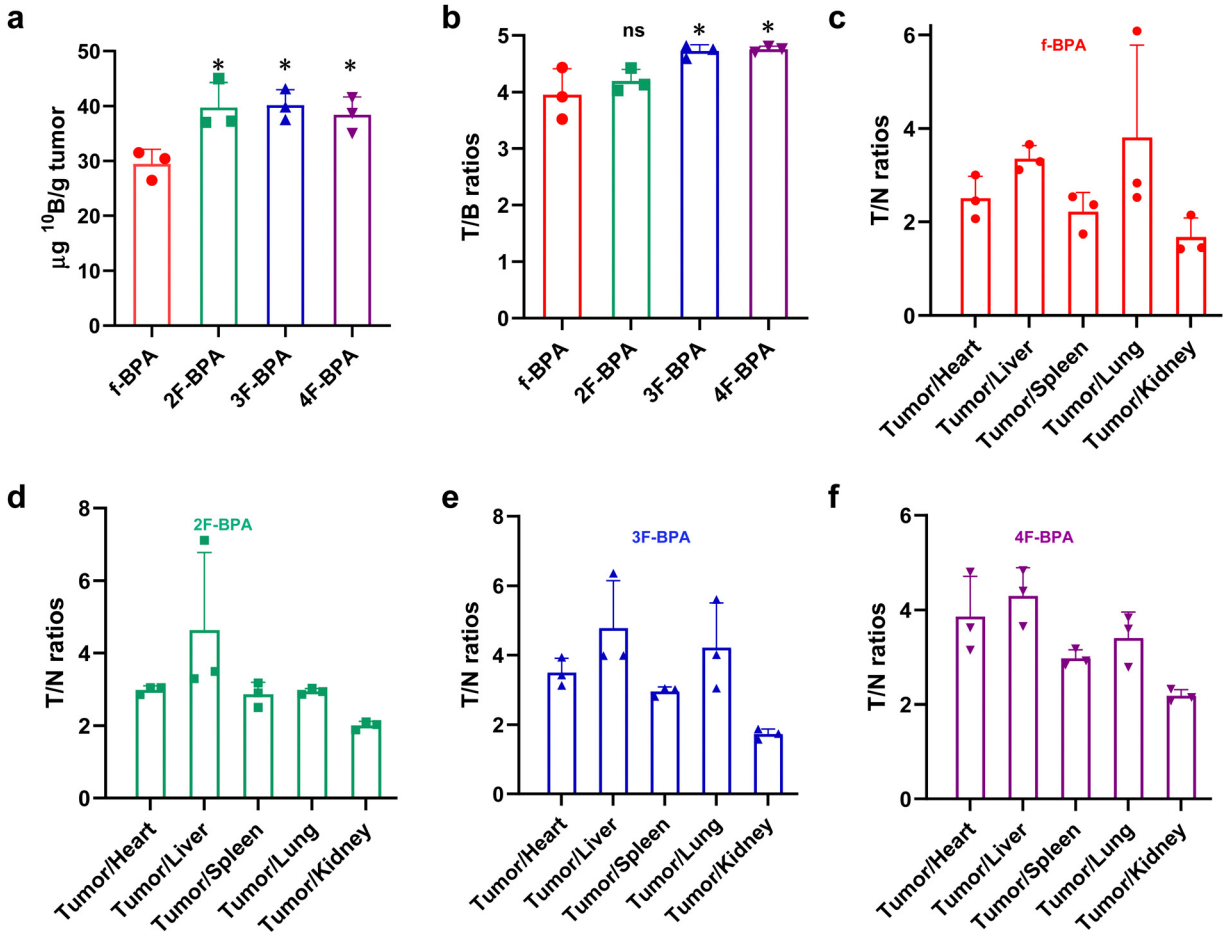

Fig. 6 *In vivo* biodistribution of f-BPA and fluorinated BPA derivatives at 2 h after intravenous injection for B16-F10 tumor-bearing mice. (a) The ^{10}B contents in tumors measured by ICP-MS for f-BPA, 2F-BPA, 3F-BPA and 4F-BPA. (b) Tumor-to-blood (T/B) ratios of f-BPA, 2F-BPA, 3F-BPA and 4F-BPA. Tumor-to-normal tissue (T/N) ratios (including the heart, liver, spleen, lungs, and kidneys) of (c) f-BPA, (d) 2F-BPA, (e) 3F-BPA and (f) 4F-BPA (ns > 0.05, *p < 0.05, **p < 0.01, ***p < 0.001 compared with f-BPA).

4F-BPA: 1.54 ± 0.10) was significantly higher than that of f-BPA (0.97 ± 0.20) (Fig. 5c). T/N is also a key to the success of BNCT. As shown in Fig. 5d–g, the T/N ratios of fluorinated BPA derivatives were significantly higher than those of f-BPA, indicating that fluorinated BPA derivatives selectively targeted tumor cells and reduced damage to surrounding normal tissues relative to f-BPA. Therefore, fluorinated BPA derivatives may become more advantageous boron delivery agents than f-BPA.

In addition, the B16-F10 tumor-bearing mouse model was also used to study the *in vivo* distribution of fluorinated BPA derivatives. As shown in Fig. 6a, the ^{10}B content in tumors reached 39.78 ± 4.52 ng per g tumor for 2F-BPA, 40.20 ± 2.83 ng per g tumor for 3F-BPA, and 38.42 ± 3.28 ng per g tumor for 4F-BPA. In contrast, the ^{10}B uptake in the surrounding normal tissues (including the heart, liver, spleen, lungs, and kidneys) and blood was relatively low (Fig. S14, ESI†). Moreover, the ^{10}B content in the tumors of fluorinated BPA derivatives was greater than that of f-BPA (28.48 ± 2.66 ng per g tumor), and there was a statistically significant difference. As shown in Fig. 6b, the T/B ratios of 3F-BPA and 4F-BPA reached 4.72 ± 0.11 and 4.76 ± 0.05, respectively, which were significantly higher than that of f-BPA (3.95 ± 0.45), suggesting that 3F-BPA and 4F-BPA are more responsive to the needs of BNCT. In addition, the T/N ratios of fluorinated BPA derivatives were also almost always greater than 3, except for the tumor-to-kidney ratios (approximately 2), which also met the requirements of clinical BNCT (Fig. 6c–f). And the T/N ratios of fluorinated BPA derivatives were higher than those of f-BPA, indicating that fluorinated BPA could better target tumor cells and decrease the harm to surrounding normal tissues.

The above experimental results showed that fluorinated BPA derivatives had higher ^{10}B accumulation in tumors and enhanced T/B and T/N ratios compared with f-BPA, which could reduce the accumulation of ^{10}B in other organs and blood, minimizing the damage to the surrounding normal tissues. Notably, the ^{10}B uptake in the tumor of fluorinated BPA derivatives in the B16-10 tumor-bearing mouse model was greater than 20 μg g^{-1} tumor, and the T/B and T/N ratios were greater than 3, showing a better delivery profile compared with the GL261 tumor-bearing mouse model, consistent with the cellular uptake results. Therefore, fluorinated BPA derivatives were more potential boron delivery agents for BNCT of B16-F10 tumors.

4. Conclusions

In summary, we developed fluorinated BPA derivatives with different fluorine groups as boron delivery agents, and the successful preparation was confirmed by ^{1}H NMR and ESI-MS results. Besides, the CCK-8 assay results suggested that fluorinated BPA derivatives had no significant cytotoxicity even at a high ^{10}B concentration of 50 ppm. Serum chemistry and hematological analysis indicated that fluorinated BPA derivatives had no significant systemic toxicity with excellent biological safety. *In vitro*, fluorinated BPA derivatives showed significantly enhanced uptake in GL261 and B16-F10 tumor cells relative to f-BPA. Furthermore, in GL261 tumor-bearing mice, although the ^{10}B accumulation in tumors for fluorinated BPA derivatives did not meet the requirements of BNCT, the ^{10}B accumulation in tumors, T/B ratio, and T/N ratio were significantly improved compared with f-BPA. Remarkably, the ^{10}B uptake in B16-F10 tumors for fluorinated BPA derivatives was higher than that for f-BPA and was much higher than the ^{10}B content required for BNCT. Compared with f-BPA, fluorinated BPA derivatives also significantly enhanced the T/B and T/N ratios, thus better targeting the tumor tissues and causing less damage to surrounding normal tissues. Therefore, fluorinated BPA derivatives would be promising boron delivery agents for clinical BNCT of tumors, especially melanoma.

Author contributions

Dandan Ding, Xueyi Wang, and Zhenhua Li designed and discussed the experiments; Dandan Ding carried out most experiments, with analytical/experimental contributions from Shushan Mo, Qishan Li, Fei Wang, Xueyi Wang, Caiwen Ou and Zhenhua Li. The manuscript draft was written by Dandan Ding with the review and editing done by Caiwen Ou and Zhenhua Li. All authors have given approval to the final version of the manuscript.

Conflicts of interest

There are no conflicts to declare.

Acknowledgements

This work was supported by the National Natural Science Foundation of China (82202307, 82202339 and 32301162), the Guangdong Basic and Applied Basic Research Foundation (2021B1515120065), and the China Postdoctoral Science Foundation (2021M701640 and 2022M711527).

References

1 R. F. Barth, J. A. Coderre, M. G. H. Vicente and T. E. Blue, *Clin. Cancer Res.*, 2005, **11**, 3987–4002.
2 R. F. Barth, A. H. Soloway and R. G. Fairchild, *Sci. Am.*, 1990, **263**, 100–107.
3 M. A. Dymova, S. Y. Taskaev, V. A. Richter and E. V. Kuligina, *Cancer Commun.*, 2020, **40**, 406–421.
4 Y. Shi, Z. Guo, Q. Fu, X. Shen, Z. Zhang, W. Sun, J. Wang, J. Sun, Z. Zhang, T. Liu, Z. Gu and Z. Liu, *Nat. Commun.*, 2023, **14**, 1884.
5 R. L. Moss, *Appl. Radiat. Isot.*, 2014, **88**, 2–11.
6 A. H. Soloway, W. Tjarks, B. A. Barnum, F.-G. Rong, R. F. Barth, I. M. Codogni and J. G. Wilson, *Chem. Rev.*, 1998, **98**, 1515–1562.
7 H. Fukuda, *Cells*, 2021, **10**, 2881.
8 P. Chang, D. Chow, L. Poisson, R. Jain and C. Filippi, *J. Neurol. Sci.*, 2017, **381**, 172–173.

9 R. F. Barth, M. G. H. Vicente, O. K. Harling, W. S. Kiger III, K. J. Riley, P. J. Binns, F. M. Wagner, M. Suzuki, T. Aihara, I. Kato and S. Kawabata, *Radiat. Oncol.*, 2012, **7**, 3–21.
10 Y. Mishima, C. Honda, M. Ichihashi, H. Obara, J. Hiratsuka, H. Fukuda, H. Karashima, T. Kobayashi, K. Kanda and K. Yoshino, *Lancet*, 1989, **334**, 388–389.
11 M. Suzuki, I. Kato, T. Aihara, J. Hiratsuka, K. Yoshimura, M. Niimi, Y. Kimura, Y. Ariyoshi, S. i Haginomori, Y. Sakurai, Y. Kinashi, S. i Masunaga, M. Fukushima, K. Ono and A. Maruhashi, *J. Radiat. Res.*, 2013, **55**, 146–153.
12 J. Li, Q. Sun, C. Lu, H. Xiao, Z. Guo, D. Duan, Z. Zhang, T. Liu and Z. Liu, *Nat. Commun.*, 2022, **13**, 2143.
13 M. Lamba, A. Goswami and A. Bandyopadhyay, *Chem. Commun.*, 2021, **57**, 827–839.
14 R. F. Barth, Z. Zhang and T. Liu, *Cancer Commun.*, 2018, **38**, 1–7.
15 J. Li, X. Wang, Z. Wang, Y. Zhao, Z. Zhang, L. Li, D. Ding, J. Guo, J. Zhang, H. Liu and Z. Li, *Biomater. Sci.*, 2023, **11**, 7568–7578.
16 L. Li, J. Li, Y. Shi, P. Du, Z. Zhang, T. Liu, R. Zhang and Z. Liu, *ACS Nano*, 2019, **13**, 13843–13852.
17 J. Li, J. Kong, S. Ma, J. Li, M. Mao, K. Chen, Z. Chen, J. Zhang, Y. Chang, H. Yuan, T. Liu, Z. Zhang and G. Xing, *Adv. Funct. Mater.*, 2021, **31**, 2100969.
18 N. Kuthala, R. Vankayala, Y. N. Li, C. S. Chiang and K. C. Hwang, *Adv. Mater.*, 2017, **29**, 1700850.
19 I. V. J. Feiner, K. R. Pulagam, K. B. Uribe, R. Passannante, C. Simó, K. Zamacola, V. Gómez-Vallejo, N. Herrero-Álvarez, U. Cossío, Z. Baz, M. M. Caffarel, C. H. Lawrie, D. J. Vugts, L. Rejc and J. Llop, *J. Mater. Chem. B*, 2021, **9**, 410–420.
20 A. Wittig, W. A. Sauerwein and J. A. Coderre, *Radiat. Res.*, 2000, **153**, 173–180.
21 P. Wongthai, K. Hagiwara, Y. Miyoshi, P. Wiriyasermkul, L. Wei, R. Ohgaki, I. Kato, K. Hamase, S. Nagamori and Y. Kanai, *Cancer Sci.*, 2015, **106**, 279–286.
22 Y. Mori, A. Suzuki, K. Yoshino and H. Kakihana, *Pigm. Cell Res.*, 1989, **2**, 273–277.
23 H. Fukuda, C. Honda, N. Wadabayashi, T. Kobayashi, K. Yoshino, J. Hiratsuka, J. Takahashi, T. Akaizawa, Y. Abe, M. Ichihashi and Y. Mishima, *Melanoma Res.*, 1999, **9**, 75–84.
24 T. Nomoto, Y. Inoue, Y. Yao, M. Suzuki, K. Kanamori, H. Takemoto, M. Matsui, K. Tomoda and N. Nishiyama, *Sci. Adv.*, 2020, **6**, eaaz1722.
25 C. Zhang, K. Yan, C. Fu, H. Peng, C. J. Hawker and A. K. Whittaker, *Chem. Rev.*, 2021, **122**, 167–208.
26 S. Ellipilli and K. N. Ganesh, *J. Org. Chem.*, 2015, **80**, 9185–9191.
27 C. Zhang, T. Liu, W. Wang, C. A. Bell, Y. Han, C. Fu, H. Peng, X. Tan, P. Král, K. Gaus, J. J. Gooding and A. K. Whittaker, *ACS Nano*, 2020, **14**, 7425–7434.
28 G. Rong, C. Wang, J. Hu, Y. Li and Y. Cheng, *J. Controlled Release*, 2022, **351**, 703–712.
29 F. Menaa, B. Menaa and O. N. Sharts, *J. Mol. Pharm. Org. Process Res.*, 2013, **1**, 2.
30 M. Wang, H. Liu, L. Li and Y. Cheng, *Nat. Commun.*, 2014, **5**, 3053.
31 L. Dafik, V. Kalsani, A. K. L. Leung and K. Kumar, *J. Am. Chem. Soc.*, 2009, **131**, 12091–12093.
32 V. Metelev, S. Zhang, S. Zheng, A. T. N. Kumar and A. Bogdanov, *Theranostics*, 2017, **7**, 3354–3368.
33 H. Huang, C. Dong, M. Chang, L. Ding, L. Chen, W. Feng and Y. Chen, *Exploration*, 2021, **1**, 50–60.
34 Y. Liu, W. Wang, D. Zhang, Y. Sun, F. Li, M. Zheng, D. B. Lovejoy, Y. Zou and B. Shi, *Exploration*, 2022, **2**, 20210274.

